Commun.Fac.Sci.Univ.Ank.Series A2-A3
Volume 61, Number 2, Pages 150-160 (2019)
DOI: 10.33769/aupse.532422
ISSN 1303-6009 E-ISSN 2618-6462
http://communications.science.ankara.edu.tr/index.php?series=A2A3

MAGNETOCALORIC EFFECT AROUND CURIE TEMPERATURE IN Ni_{50-x} $Cu_xMn_{38}Sn_{12}B_3$ SHAPE MEMORY RIBBONS

Olcay KIZILASLAN

ABSTRACT. The magnetocaloric effect in $Ni_{50-x}Cu_xMn_{38}Sn_{12}B_3$ ribbons depending on the Cu substitution (x= 0, 1, 3) was investigated around the Curie temperature. The purpose of the present study was to analyze the magnetocaloric effect around a second order phase transition (around the Curie temperature) which has a smaller thermal hysteresis compared to a first order phase transition (Martensitic transition). The Curie temperature of the ribbons shifted to higher temperatures with increasing Cu content. A conventional magnetocaloric effect (MCE) was observed around the Curie temperature when the ribbons are subjected to a magnetic field change of 5 T. The magnetic entropy changes were calculated based on the isothermal magnetization M(H) data using thermodynamic Maxwell equation. The highest magnetic entropy change and the refrigerant capacity was obtained for the x=1 ribbon.

1. INTRODUCTION

Ni-Mn-X (X = Sn, In and Sb) metamagnetic shape memory alloys (MSMAs) are of great interests due to their potential applications such as magnetic refrigeration materials, magnetic shape memory effect, magneto-resistance, magneto-thermal conductivity, elasta-caloric effect [1-11]. These alloys are one step ahead in practical applications when considering the cost-performance relationship [12]. They have also a large refrigeration capacity (RC) around martensitic-austenite phase transition [13] which is comparable to the compounds containing rare-earth element [14,15]. Strong conventional magnetocaloric effect (MCE) is caused by a magnetic transition since the magnetization strongly varies in a very narrow temperature range around transition temperature. The MCE can be tuned [16,17] by substituting or doping ferromagnetic [18-20] or non-ferromagnetic elements [21-23].

Received by the editors: February 26, 2019; Accepted: June 25, 2019.
Key word and phrases: Ni-Mn-Sn Heusler alloys, magnetocaloric effect, magnetic properties, substitution.

The total adiabatic entropy change of a magnetic material is the sum of magnetic ΔS_M, lattice ΔS_L, and electronic ΔS_E entropy given by $\Delta S_T = \Delta S_M + \Delta S_L + \Delta S_E$. The lattice and electronic entropy are independent of external magnetic field. The total entropy is constant if the process is adiabatic and reversible. When a magnetic field is applied on the material, the magnetic moments of the material are aligned along the magnetic field direction which implies a decrease in magnetic entropy. For the conservation of total entropy change, the decrease in the magnetic entropy is compensated by an increase in the lattice entropy. The increase in lattice entropy causes an increase of the material temperature.

This study investigates the effect of Cu substitution on magnetocaloric effect in the vicinity of Curie temperature (T_C) in $Ni_{50-x}Cu_xMn_{38}Sn_{12}B_3$ (x = 0, 1, 3) shape memory ribbons. The Curie temperatures for x = 0, 1, 3 were found to be 315, 321 and 319 K, respectively, which are very close to room temperature. This makes the investigation of the MCE around the Curie temperature important. On the other hand, the transition around the curie temperature is a second order phase transition and this will be discussed below. Such a transition provides a large usable temperature range (compared to a first order transition [24] observed in this compound at low temperature) as the transition temperature of the ribbon has to span the entire working region of the cooling device. The MCE and the effective refrigerant capacity RC_{eff} were calculated depending on the Cu substitution. The magnetic entropy change ΔS_M was determined on the basis of magnetization data $M(H)$. The highest RC value (96.44 J/kg) was found for the x=3.

This study investigates the effect of Cu substitution on magnetocaloric effect in the vicinity of Curie temperature (T_C) in Ni_{50}-x$Cu_xMn_{38}Sn_{12}B_3$ (x = 0, 1, 3) shape memory ribbons. The Curie temperatures for x = 0, 1, 3 were found to be 315, 321 and 319 K, respectively, which are very close to room temperature. This makes the investigation of the MCE around the Curie temperature important. On the other hand, the transition around the curie temperature is a second order phase transition and this will be discussed below. Such a transition provides a large usable temperature range (compared to a first order transition [24] observed in this compound at low temperature) as the transition temperature of the ribbon has to span the entire working region of the cooling device. The MCE and the effective refrigerant capacity RC_{eff} were calculated depending on the Cu substitution. The magnetic

entropy change ΔS_M was determined on the basis of magnetization data $M(H)$. The highest RC value (96.44 J/kg) was found for the x=3.

2. Experimental

The appropriate amount of Ni, Mn, Sn, B and Cu powders were mixed to fabricate $Ni_{50-x}Cu_xMn_{38}Sn_{12}B_3$ (x = 0, 1, 3) shape memory ribbons and the mixture was melted in an arc-melter in an argon atmosphere. Thus, the ignots of the polycrystalline $Ni_{50-x}Cu_xMn_{38}Sn_{12}B_3$ were produced. In order to make the ingots more homogeneous, the melting process was repeated several times. The obtained ingots were used to produce the ribbons by melt-spinning technique. The dimensions of the produced ribbons were about 5-6 mm in width, 20-25 mm in length and 15-20 μm in thickness, respectively. The ribbons were also heat treated in vacuumed quartz ampoules at 1173 K for 2 h and then quenched in ice-water.

Magnetic measurements were performed with Quantum Design Physical Property Measurement System (PPMS) - 9T. The system is able to resolve the magnetization changes of less than 10^{-6} emu at a data rate of 1 Hz. The sweep rate, which means how fast the magnetic field change between the field set points, was set to 100 Oe/sec for all the measurement.

3. Results and discussion

Figure 1 shows the magnetization-temperature (M-T) curves of the ribbons under a magnetic field of 1T. A magnetic transition (MT) from a ferromagnetic state to a paramagnetic state was observed. Curie temperatures T_C were obtained to be 315, 320 and 317 K for x= 0, 1 and 3, respectively. T_C values were determined by taking the first derivative of M(T) curves. The increase of the Curie temperature is attributed to the enhancement of ferromagnetic coupling.

Figure 2a shows the isothermal M-H curves of the x= 0 parent ribbon at the temperatures from 300 to 360 K in an interval of 5 K. The measurements were performed at the temperatures in the vicinity of the Curie temperature. A similar $M(H)$ characteristic was also observed for the x=1 and 3 ribbons.

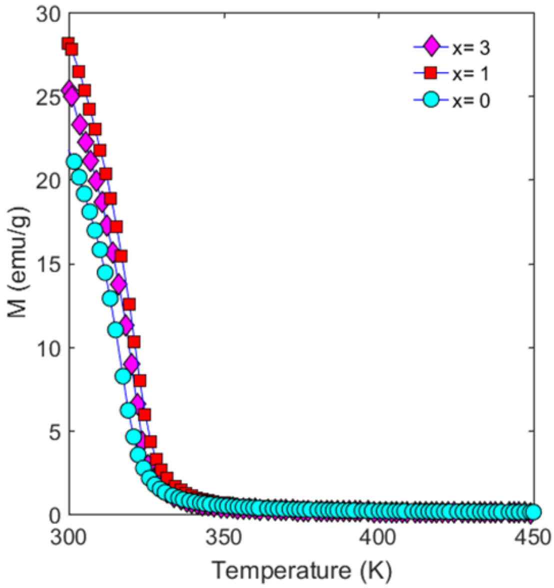

FIGURE 1. The magnetization curve of the samples as a function of temperature at the magnetic field of 1 T.

The Arrott plot technique was used to determine the nature of magnetic phase transition. Figure 2b shows M^2 versus H/M curves obtained from $M(H)$ data (figure 2a) at the temperatures around the Curie temperature. According to Banerjee's criterion [25], if the slope is positive, the material undergoes a second order phase transition (SOPT). Figure 2b clearly indicates that the ribbons used in this study undergo a second order phase transition around the Curie temperature. For the x=1 and 3 Cu substituted ribbons, a similar Arrott plot characteristic was observed. As the transition around the Curie temperature is a second order phase transition, there exists a small thermal hysteresis. A large thermal hysteresis generally accompanies to the first order magnetic phase transition and this strongly influences the refrigerant efficiency of the MCE. It should be emphasized that the thermal hysteresis increases the temperature range of refrigeration cycle, causing a reduce in the refrigerant efficiency [26]. On this purpose, in this study the MCE properties of Ni_{50-x} $Cu_xMn_{38}Sn_{12}B_3$ ribbons were investigated around the Curie temperature. The magnetocaloric efficiency around a transition with small thermal hysteresis is much higher and the corresponding MCE can be more effectively used in the magnetic refrigeration technology. It is worth to note that the MCE was generally investigated in the literature around the martensitic transition which has very large thermal hysteresis. For the $Ni_{50-x}Cu_xMn_{38}Sn_{12}B_3$ ribbons there is no study reported in the literature on the investigation of the MCE around the Curie temperature.

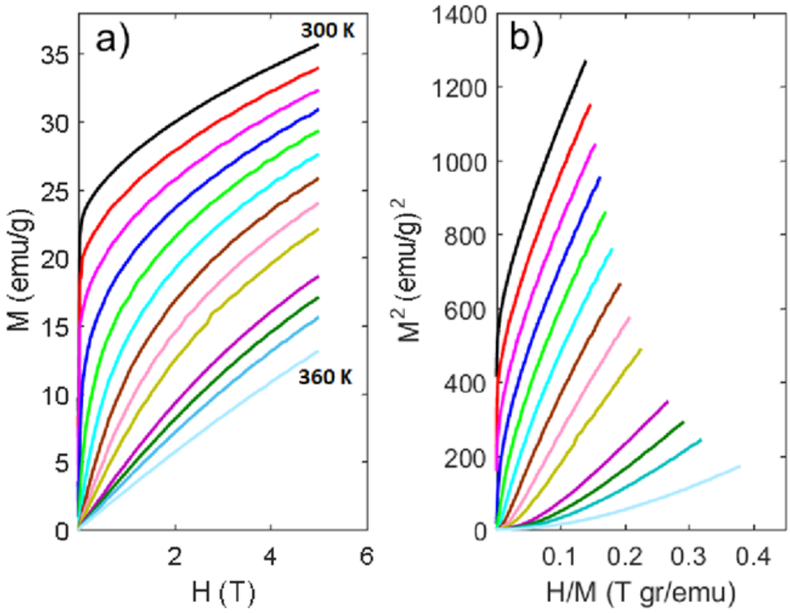

FIGURE 2. a) the M-H curves of the ribbon (x=0) up to 5T, at different temperatures between 300 K and 360K in an interval of 5K, b) Arrott (M^2 vs H/M) plots.

Magnetic entropy change can be calculated by using the following thermodynamic Maxwell equation;

$$\Delta S_M = \int_{H_O}^{H_F} \left(\frac{\partial M}{\partial T}\right)_H dH \qquad \text{Eq. 1}$$

where $H_0 = 0$, if the field is changed from 0 to H. $\frac{\partial M}{\partial T}$ can be calculated numerically with a simple formula given below, Eq. 2. The integral was numerically solved using the trapezoidal integration.

$$\frac{\partial M}{\partial T} = \sum_{i=1}^{i_{max}} \frac{M(T_{i+1}) - M(T_i)}{T_{i+1} - T_i} \qquad \text{Eq. 2}$$

If the number of experimental $M(H)$ curves is N (an integer number), the resulting $\Delta S_M - T$ data will have N-1 points. The reason for this loss is the numerical method used for the calculation of the derivative, see eq.2.

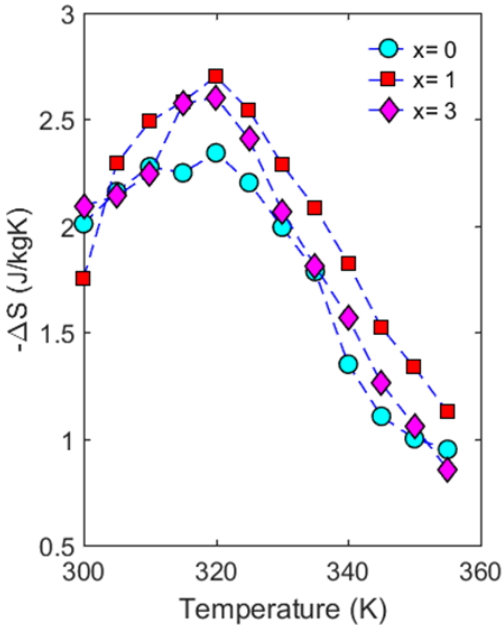

FIGURE 3. Temperature dependence of the isothermal magnetic entropy change change ΔS_M at different at different Cu substitution levels under a magnetic field change of 5 T.

Figure 3 shows ΔS_M as a function of temperature calculated by using Eq. 1 at different substitution levels (x= 0, 1 and 3). The measurements were performed at the temperatures below and above Curie temperature (T_c) with the temperature steps of ΔT=5 K. The ΔS_M^{max} values were calculated to be 2.34, 2.71 and 2.60 J/kgK for the x=0, 1 and 3 ribbons, respectively, indicating an increase in ΔS_M^{max} of 15.8 % for the x= 1 ribbon compared to the x=0 ribbon.

The magnetization difference, ΔM, between two phases is responsible for magnetic entropy change [27]. If one wants to improve ΔS_M, the magnetization difference ΔM should be tuned. In the present study, the magnetization was increased by substituting Cu for Ni, see figure 1. Magnetic properties of Heusler alloys are very sensitive to the structural disorder and strongly depends on the exchange interaction between Mn-Mn atoms [28] because the contribution of the magnetic moments of Ni atoms to the total magnetic moment in Ni-Mn-X (X=Sn, Sb, In) alloys is quite low [29,30]. The exchange interaction determines whether the magnetic order is ferromagnetic or antiferromagnetic. The substitution of Cu for Ni causes a change of the distances between Mn-Mn atoms. These new interatomic distances are more favorable for the ferromagnetic order. Therefore, the Cu substitution leads to a strong ferromagnetic coupling. Figure 1 supports this idea and an increase in the magnetization difference ΔM was observed in the x=1 and 3 ribbons. The ΔM value is decreased in the x=3 ribbon compared to the x=1 ribbon but it was still bigger than the ΔM value of the x=0 parent ribbon.

A large refrigerant capacity value RC as well as large entropy change is also crucial parameter for the magnetic refrigeration applications. The area under $\Delta S_M - T$ curve in Figure 3 gives the refrigerant capacity $\left(RC = \int_{T_1}^{T_2} \Delta S_M \, dT\right)$, which is a measurement of heat transport between hot and cold reservoirs in an ideal refrigerator. T_1 and T_2 are the temperatures which correspond to half maximum value (ΔT_{FWHM}) in both side of ΔS_M peak. The area was calculated by trapezoidal integration method and the corresponding RC versus x is given in Figure 4. The highest RC value was found to be 88.89 J/kg for the x=1 which indicates an increase of RC by 13.7 %. The maximum RC obtained in this study is comparable with the other Heusler alloys [26,31-34].

Hysteresis loss (HL) must be taken into account for evaluating effective refrigerant capacity RC_{eff} during a thermodynamic cycle. The area between magnetization and demagnetization curves gives HL. The RC_{eff} can be calculated by subtracting hysteresis loss from RC, $RC_{eff} = RC - HL$ [27]. The calculated hysteresis areas at 335 K for the x=0, 1 and 3 were very small and found to be 0.59, 0.66 and 1.05 J/kg for the x=0 ,1 and 3, respectively. Then, the calculated RC_{eff} values are 77.58, 88.24 and 82.2 J/kg for the x= 0, 1 and 3, respectively. The obtained RC_{eff} values are comparable with the other Ni-Mn-Sn systems, see figure 8 in ref [27] and a promising value for the magnetocaloric applications in the future.

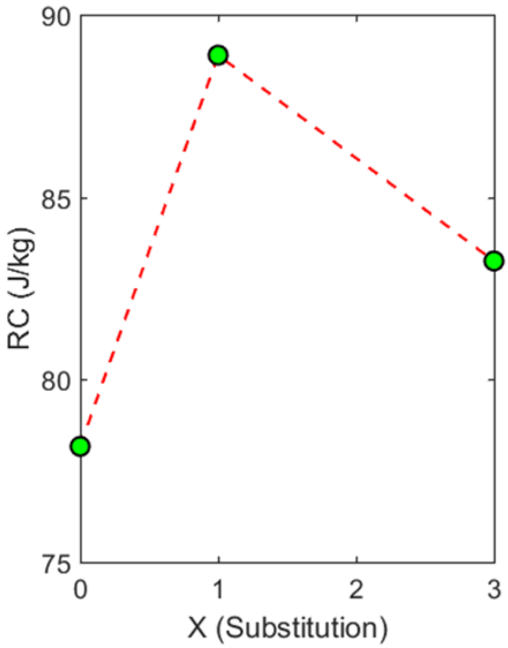

FIGURE 4. The calculated refrigerant capacity, RC, for different substitution levels.

4. Conclusion

In this study, the effect of Cu substitution on the magnetocaloric effect and Curie temperature was investigated. The Cu substitution helped to tune not only the magnetocaloric effect also the Curie temperature. An increase of 6 K was observed in the Curie temperature of the x=1 ribbon. However, a decrease in the Curie temperature of the x= 3 ribbon was observed, but it was still above the Curie temperature of the x= 0 parent ribbon. For the x=1 ribbon, a significant magnetic entropy change (ΔS_M^{max}= 2.71 J/kgK) was obtained under a magnetic field change of 5 T. The highest RC_{eff} value, which is a better criterion to evaluate the cooling efficiency, was obtained to be 88.89 J/kg for the x=1.

References

[1] Aydogdu, Y. , Turabi, A.S., Aydogdu, A., Kok, M., Yakinci, Z. D., Karaca, H. E.: The effects of boron addition on the magnetic and mechanical properties of NiMnSn shape memory alloys, J. Therm. Anal. Calorim. 126, (2016), 399–406.

[2] Zhang, B., Zhang, X., Yu, S. , Chen, J., Cao, Z. , Wu, G.: Giant magneto thermal conductivity in the Ni–Mn–In ferromagnetic shape memory alloys, Appl. Phys. Lett. 91, (2007), 012510.

[3] Castillo-Villa, P.O., Mañosa, L., Planes, A., Soto-Parra, D.E., Sánchez-Llamazares, J.L., Flores-Zúñiga, H., and Frontera, C.: Elastocaloric and magnetocaloric effects in Ni-Mn-Sn (Cu) shape-memory alloy, J. Appl. Phys. 113, (2013), 053506.

[4] Pramanick, S., Chatterjee, S., Giri, S., Majumdar, S., Koledov, V. V., Mashirov, A., Aliev, A. M., Batdalov, A. B., Hernando, B., Rosa, W. O., and Gonzlez-Legarreta, L.: Multiple magneto-functional properties of $Ni_{46}Mn_{41}In_{13}$ shape memory Alloy, J. Alloys Compd. 578, (2013), 157161.

[5] Samanta, T., Saleheen, A. U., Lepkowski, D. L., Shankar, A., Dubenko, I., Quetz, A., Khan, M., Ali, N. and Stadler, S.: Asymmetric switchinglike behavior in the magnetoresistance at low fields in bulk metamagnetic Heusler alloys, Phys. Rev. B. 90, (2014), 064412.

[6] Yu, S. Y., Liu, Z. H., Liu, G. D., Chen, J. L., Cao, Z. X., Wu, G. H., Zhang, B., and Zhang, X.: Large magnetoresistance in single-crystalline $Ni_{50}Mn_{50-x}In_x$ alloys, x= (14–16) upon martensitic transformation, Appl. Phys. Lett. 89, (2006), 162503.

[7] Sutou, Y., Imano, Y., Koeda, N., Omori, T., Kainuma, R., Ishida, K. and Oikawa, K.: Magnetic and martensitic transformations of NiMnX(X=In,Sn,Sb) ferromagnetic shape memory alloys, Appl. Phys. Lett. 85, (2004), 4358.

[8] Krenke, T., Acet, M., Wassermann, E. F., Moya, X., Manosa, L., and Planes, A.: Ferromagnetism in the austenitic and martensitic states of Ni-Mn-In Alloys, Phys. Rev. B. 73, (2006), 174413.

[9] Manosa, L., Alonso, D. G., Planes, A., Bonnot, E., Barrio, M., Tamarit, J. L., Aksoy, S. and Acet, M.: Giant solid-state barocaloric effect in the Ni-Mn-In magnetic shape-memory alloy, Nat. Mat. 9, (2010), 478–481.

[10] Kirat G, Kizilaslan O, Aksan M. A.: Magnetoresistance properties of magnetic Ni-Mn-Sn-B shape memory ribbons and magnetic field sensor aspects operating at room temperature. J. Magn. Magn. Mater. 477, (2019), 366-371.

[11] Chattopadhyay, M. K., Manekar, M. A., Sharma, V. K., Arora, P., Tiwari, P., Tiwari, M. K. and Roy, S. B.: Contrasting magnetic behavior of $Ni_{50}Mn_{35}In_{15}$ and $Ni_{50}Mn_{34.5}In_{15.5}$ Alloys, J. Appl. Phys. 108, (2010), 073909.

[12] Chen, F., Liu, W.L., Shi, Y.G., Müllner, P.: Influence of annealing on martensitic transformation and magnetic entropy change in $Ni_{37.7}Co_{12.7}Mn_{40.8}Sn_{8.8}$ magnetic shape memory alloy ribbon, J. Magn. Magn. Mater. 377, (2015), 137–44.

[13] Huang, L., Cong, D. Y., Suo, H. L. and Wang, Y. D.: Giant magnetic refrigeration capacity near room temperature in $Ni_{40}Co_{10}Mn_{40}Sn_{10}$ multifunctional alloy. Appl. Phys. Lett. 104, (2014),132407.

[14] Gschneidner K. A., and Pecharsky, V. K.: Magnetocaloric Materials, Annual Rev. Mater. Sci. 30, (2000), 387–429.

[15] Khattak, K. S., Aslani, A., Nwokoye, C. A., Siddique, A., Bennett, L. H., and Torre, E. D.: Magnetocaloric properties of metallic nanostructures, Cogent Engineering 2, (2015), 1050324.

[16] Liu, J., Scheerbaum, N., Lyubina, J. and Gutfleisch, O.: Reversibility of magnetostructural transition and associated magnetocaloric effect in Ni-Mn-In-Co., Appl. Phys. Lett. 93, (2008), 102512.

[17] Zhang, Y. et al.: Large magnetic entropy change and enhanced mechanical properties of Ni-Mn-Sn-C alloys., Scripta Mater. 75, (2014), 26–29.

[18] Tan, C., Tai, Z., Zhang, K., Tian, X. and Cai, W.: Simultaneous enhancement of magnetic and mechanical properties in Ni-Mn-Sn alloy by Fe doping., Sci. Rep. 7, (2017), 43387.

[19] Tan, C. L., Feng Z. C., Zhang, K., Wu, M. Y., Tian, Guo E. J.: Microstructure, martensitic transformation and mechanical properties of Ni-Mn-Sn alloys by substituting Fe for Ni, Trans. Nonferrous Met. Soc. China. 27, (2017), 2234–2238.

[20] Zhang, H. H., Zhang, X., Qian, M., Wei, L., Xing, D., Sun, J., Geng, L.: Enhanced magnetocaloric effects of Ni-Fe-Mn-Sn alloys involving strong metamagnetic behavior. J. Alloy. Compd. 715, (2017), 206–213.

[21] Qu, Y.H., Cong, D.Y., Sun X.M., Nie Z.H., Gui, W.Y., Li R.G., Ren Y., Wang, Y.D..: Giant and reversible room-temperature magnetocaloric effect in Ti-doped Ni-Co-Mn-Sn magnetic shape memory alloys. Acta Mater. 134, (2017), 236–248.

[22] Cong, D. Y., Huang, L., Hardy, V., Bourgault, D., Sun, X. M., Nie, Z.H., Wang, M.G., Ren, Y., Entel, P., Wang, Y. D.: Low-field-actuated giant magnetocaloric effect and excellent mechanical properties in a NiMn-based multiferroic alloy. Acta Mater. 146, (2018), 142–151.

[23] Liu, C., Li, Z., Zhang, Y., Liu, Y., Sun., J., Huang., Y., Kang, B., Xu, K., Deng, D., Jing, D.: Martensitic transition, inverse magnetocaloric effect and shape memory characteristics in $Mn_{48-x}Cu_xNi_{42}Sn_{10}$ Heusler alloys. Phys. Rev. B Condens. Matter. 508, (2017), 118–123.

[24] Kizilaslan, O., Thermal hysteresis dependent magnetocaloric effect properties of $Ni_{50-x}Cu_xMn_{38}Sn_{12}B_3$ shape memory ribbons, Intermetallics 109, (2019), 135–138.

[25] B.K.Banerjee, On a generalised approach to first and second order magnetic transitions, Phys. Lett. 12, (1964),16.

[26] Tian, F. Zeng, Y, Xu, M., Yang, S., Lu, T, Wang, J., Chang, T, Adil, M., Zhang, Y, Zhou, C. and Song, X.: A magnetocaloric effect arising from a ferromagnetic transition in the martensitic state in Heusler alloy of $Ni_{50}Mn_{36}Sb_8Ga_6$, Appl. Phys. Lett. 107, 012406 (2015).

[27] Zhang, X., Zhang, H., Qian, M. and Geng, L.: Enhanced magnetocaloric effect in Ni-Mn-Sn-Co alloys with two successive magnetostructural transformations Sci. Rep. 8, (2018), 8235.

[28] Hernando, B., Sanchez Llamazares, J.L., Santos, J.D., Sanchez, M.L., Escoda, Ll., Sunol, J.J., Varga, R., Garcia, C., Gonzalez, J.: Grain oriented NiMnSn and NiMnIn Heusler alloys ribbons produced by melt spinning: Martensitic transformation and magnetic properties, J. Magn. Magn. Mater. 321, (2009), 763–768.
[29] Luo, H., Meng, F., Jiang, Q., Liu, H., Liu, E., Wu G. and Wang, Y.: Effect of boron on the martensitic transformation and magnetic properties of $Ni_{50}Mn_{36.5}Sb_{13.5-x}B_x$ alloys, Scripta Mater. 63 (2010), 569–572.
[30] Kübler, J., William, A. R., and Sommers, C. B.: Formation and coupling of magnetic moments in Heusler alloys, Phys. Rev. B. 28, (1983), 1745.
[31] Pecharsky, V. K. Gschncidner K. A. Jr.: Giant Magnetocaloric Effect in $Gd_5(Si_2Ge_2)$, Phys. Rev. Lett. 78, (1997) 4494.
[32] Khan, M., Ali, N., Stadler, S.: Inverse magnetocaloric effect in ferromagnetic $Ni_{50}Mn_{37+x}Sb_{13-x}$ Heusler alloys J. Appl. Phys. 101 (2007), 053919.
[33] Varzaneh, A. G., Kameli, P., Amiri, T., Ramachandran, K.K., Mar, A., Sarsari, I. A., Luo, J. L., Etsell, T. H., Salamati, H.: Effect of Cu substitution on magnetocaloric and critical behavior in $Ni_{47}Mn_{40}Sn_{13-x}Cu_x$ alloys, J. Alloy. Compd., 708, (2017) 34-42.
[34] Zhang, Y., Zheng, Q., Xia, W., Zhang, J., Dua, J., and Yana, A.: Enhanced large magnetic entropy change and adiabatic temperature change of $Ni_{43}Mn_{46}Sn_{11}$ alloys by a rapid solidification method, Scripta Mater. 104, (2015) 41–44.

Current Address: Olcay KIZILASLAN: Inonu University, Department of Biomedical Engineering, Faculty of Engineering 44280, Malatya, Turkey
E-mail: olcay.kizilaslan@inonu.edu.tr, olcaykizilaslan@gmail.com
Orcid ID: https://orcid.org/0000-0003-2528-433X